

NEAR 3:2 AND 2:1 MEAN MOTION RESONANCES FORMATION IN THE SYSTEMS OBSERVED BY KEPLER

SU WANG¹ AND JIANGHUI JI¹

Draft version July 23, 2018

ABSTRACT

The Kepler mission has released ~ 4229 transiting planet candidates. There are approximately 222 candidate systems with three planets. Among them, the period ratios of planet pairs near 1.5 and 2.0 reveal that two peaks exist for which the proportions of the candidate systems are $\sim 7.0\%$ and 18.0% , respectively. In this work, we study the formation of mean motion resonance (MMR) systems, particularly for the planetary configurations near 3:2 and 2:1 MMRs, and we concentrate on the interplay between the resonant configuration and the combination of stellar accretion rate, stellar magnetic field, speed of migration and additional planets. We perform more than 1000 runs by assuming a system with a solar-like star and three surrounding planets. From the statistical results, we find that under the formation scenario, the proportions near 1.5 and 2.0 can reach 14.5% and 26.0% , respectively. In addition, $\dot{M} = 0.1 \times 10^{-8} M_{\odot} \text{ yr}^{-1}$ is propitious toward the formation of 3:2 resonance, whereas $\dot{M} = 2 \times 10^{-8} M_{\odot} \text{ yr}^{-1}$ contributes to the formation of 2:1 resonance. The speed-reduction factor of type I migration $f_1 \geq 0.3$ facilitates 3:2 MMRs, whereas $f_1 \geq 0.1$ facilitates 2:1 MMRs. If additional planets are present in orbits within the innermost or beyond the outermost planet in a three-planet system, 3:2:1 MMRs can be formed, but the original systems trapped in 4:2:1 MMRs are not affected by the supposed planets. In summary, we conclude that this formation scenario will provide a likely explanation for Kepler candidates involved in 2:1 and 3:2 MMRs.

Subject headings: (stars:) planetary systems-planets and satellites: formation-methods: numerical

1. INTRODUCTION

The Kepler mission has released data spanning over 16 months (Fabrycky et al. 2012; Batalha et al. 2013; Mazeh et al. 2013). The statistical results, obtained from 361 multiple-planet systems, show that there are two peaks for the period ratios of two planets in a system: approximately 1.5 and 2.0. This finding may provide evidence that there are a plenty of planet pairs near 3:2 mean motion resonances (MMRs) (with the period ratio of two planets in the range of [1.45, 1.54]) and 2:1 MMRs (with the period ratio of two planets in the range of [1.83, 2.18]) (Lissauer et al. 2011). As of July 2014, approximately 4229 planet candidates have been reported in 2804 planetary systems, most of which will be subsequently confirmed as authentic planets through follow-up observations and by double checking the data. In this population, there are 974 multiple planetary systems, including 652 two-planet systems, 222 three-planet systems and 75 four-planet systems. As previously mentioned, most of the planetary candidates in the multiple planetary systems are believed to be real planets (Lissauer et al. 2012; Ciardi et al. 2013; Quillen et al. 2013). Based on current data, in Figure 1, we show the distribution of the period ratios of the planet pairs for all of the planetary candidates (*the upper panel*) and for all of the three-planet systems (*the lower panel*). The upper panel shows that the proportion of the period ratios for two planets near 1.5 ($\sim 10.5\%$) and 2.0 ($\sim 20.5\%$) appear to be much larger than the proportion of other period ratios. In contrast, the lower panel shows that two peaks are also observed for the case of three-planet

systems (see Fig.1) in which the proportions of systems near 1.5 and 2.0 are approximately 7.0% and 18.0% , respectively. Furthermore, we note that two peaks occur at period ratios greater than the exact values of 1.5 and 2.0. Such a distribution may be related to planets near 4:2:1 MMRs (so-called Laplacian resonances) or 3:2:1 MMRs.

These observations indicate that a great many systems are approximately involved in MMR (Figure 1). Therefore, investigation into the formation scenarios of such resonant configurations should inform planetary formation theory in several respects. Currently, several formation scenarios are proposed to explain the formation of systems near MMRs.

First, it is difficult for planet candidates observed by Kepler to form in situ based on the Minimum Mass Solar Nebula (MMSN) model (Hayashi 1981). For all planetary candidates, the planetary radii are in the range of $[0.24, 154] R_{\oplus}$ with an average value of $2.09 R_{\oplus}$, whereas the radii of the planets in three-planet systems range from 0.31 to $26 R_{\oplus}$ with an average value of $1.92 R_{\oplus}$. In addition, for three-planet systems, $\sim 75\%$ of the planetary radii are in the range of $[1, 3] R_{\oplus}$ with semi-major axes that are shorter than 1.14 AU. A recent investigation of the internal structure of terrestrial and Neptune-like planets indicates that a planet's mass radius follows the relationship $R \propto M^{0.226-0.262}$ (Valencia et al. 2006, 2007; Marcus et al. 2010; Howard 2013; Lee et al. 2013). Thus, the planets have average masses in the range of $[12, 18] M_{\oplus}$. Considering an isolation mass m_{iso} in a core-accretion model (Ida & Lin 2004), to yield a planet with the average mass and radius of a three-planet system, the enhancement factor of the MMSN should be greater than 16. Hence, it is difficult to explain the final configuration of multiple-planet systems based on an in

¹ Key Laboratory of Planetary Sciences, Purple Mountain Observatory, Chinese Academy of Sciences, Nanjing 210008, China; wangsu@pmo.ac.cn, jjjh@pmo.ac.cn.

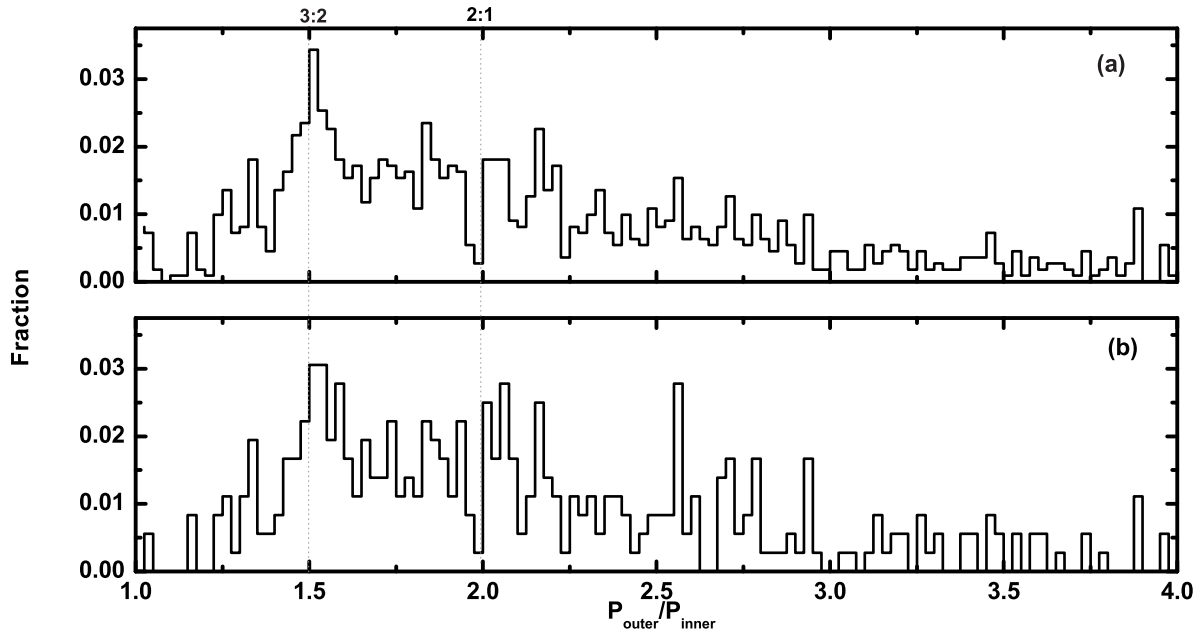


FIG. 1.— The statistical results of planet pairs in Kepler systems. Upper panel shows the period ratio of two planets for all planetary candidates, whereas the lower panel represents the values simply for three-planet systems. Two grey dotted lines are associated with exact 3:2 and 2:1 MMRs.

situ-formation scenario.

The most classical theory for producing such a configuration is the convergent migration scenario that occurs in the gaseous disk (Goldreich & Tremaine 1980; Lin et al. 1996). Given an appropriate orbital migration speed, two planets can easily be captured in MMR (Bryden et al. 2000; Masset & Snellgrove 2001). Systems such as GJ 876, with two planets of a four-planet system captured in a 2:1 MMR (Lee & Peale 2002; Ji et al. 2002, 2003; Zhou et al. 2005; Zhang et al. 2010), and KOI-152, which consists of three companions in a near-Laplacian configuration (Wang et al. 2012), are well explained via this migration scenario, and the KBOs which are captured with Neptune in 3:2 or 2:1 MMRs are demonstrated by the migration of Neptune (Malhotra 1995).

An alternative scenario is proposed (Petrovich et al. 2013) to elucidate the formation of near-MMR for systems with growing-mass planets. In this case, the authors show that the 3:2 resonance is the strongest first-order resonance for a planet with a mass of 20-100 M_{\oplus} . However, the effects of dissipation orbital migration are not fully taken into account in the authors' work, which may play a significant role in the capture of resonant planets, especially for a 2:1 MMR.

Recently, Ogihara & Kobayashi (2013), using numerical simulations, investigated the formation scenario that triggered two planets to capture a first-order MMR. In their work, the authors also considered the combination of orbital migration and gas damping. For two well-separated planets, the planets may undergo convergent migration and may ultimately become trapped in MMR during their evolution, whereas for closely spaced planet pairs, the planets may be formed in situ. In their simulations, the authors explored simple systems with two

equal-mass planets. Nevertheless, the formation scenario in a three-planet system would be quite different because of the gravitational perturbation caused by the third planet. Moreover, the planetary mass ratio acts as an alternative factor in shaping the final configuration of the system. In-depth investigation is required to understand planetary formation in packed systems.

Based on our former study (Wang et al. 2012) and observational data, our main aim in this work is to determine the formation scenario that may lead to the various types of MMR that match statistical outcomes by taking three-planet systems as an example. In our simulations, we consider three planets whose masses are lower than 30 M_{\oplus} . These low-mass planets are believed to form at a distant region rather than at their present locations; thus, they will undergo type I migration until they reach the inner region of the gaseous disk and stop migrating. Subsequently, tidal interactions between the planets and the central star will circularize their resultant orbits. Such a formation process is mainly affected by three important factors: the speed of the type I migration, the stellar magnetic field, and the stellar accretion rate, which may shape the final configuration of the investigated systems. Moreover, the stellar magnetic field and stellar accretion rate affect the density profile of the gaseous disk (Kretke & Lin 2007; Kretke et al. 2009; Wang et al. 2012), which also plays an important role in determining each planet's final location.

In this work, we focus on the configuration formation of near-MMR, particularly 3:2 and 2:1 MMRs, in three-planet systems as a function of (1) the speed of the type I migration based on the value obtained by linear analysis, (2) the stellar accretion rate from early to later stages, (3) the stellar magnetic field, and (4) the potential sur-

vival of additional planets in the systems that may break up the MMRs. In Section 2, we summarize our models, including the disk model and the migration scenario that planets may experience. Section 3 presents the numerical results obtained for two different cases of planet configuration. Section 4 presents our discussion and conclusions.

2. MODELS

2.1. Disk Model

The surface density of a gas disk at a stellar distance a is described as (Pringle 1981)

$$\Sigma_g = \frac{\dot{M}}{3\pi\alpha(a)c_s h} \exp\left(\frac{-t}{\tau_{\text{dep}}}\right) \eta, \quad (1)$$

where t is time, the timescale τ_{dep} is estimated to be approximately several million years (Haisch et al 2001) and c_s and h are the speeds of sound at the midplane and isothermal density scale height, respectively. Herein, \dot{M} is the stellar accretion rate, which can be evaluated as (Natta et al. 2006; Vorobyov & Basu 2009)

$$\dot{M} \simeq 2.5 \times 10^{-8} \left(\frac{M_*}{M_\odot}\right)^{1.3 \pm 0.3} M_\odot \text{ yr}^{-1}. \quad (2)$$

For a star with a solar mass, the stellar accretion rate is $\sim 2.5 \times 10^{-8} M_\odot \text{ yr}^{-1}$. The average value of this rate decreases as the star and the disk evolve. Thus, herein, we suppose that the stellar accretion rate varies from 0.1×10^{-8} to $2.5 \times 10^{-8} M_\odot \text{ yr}^{-1}$ **representing different stage of the star evolution** for a solar-like system. In addition, the efficiency factors of angular momentum transport α and η are defined as

$$\alpha_{\text{eff}}(a) = \frac{\alpha_{\text{dead}} - \alpha_{\text{mri}}}{2} \left[\text{erf}\left(\frac{a - a_{\text{crit}}}{0.1a_{\text{crit}}}\right) + 1 \right] + \alpha_{\text{mri}}, \quad (3)$$

$$\eta = 0.5 \left[\text{erf}\left(\frac{a - a_{\text{mstr}}}{0.1a_{\text{mstr}}}\right) + 1 \right], \quad (4)$$

where a_{crit} and a_{mstr} are the locations of the boundary of magneto-rotational instability (MRI) and the truncation of the magnetic field, respectively. Specifically, the two parameters are modeled as (Kretke et al. 2009; Koenigl 1991)

$$a_{\text{crit}} = 0.16 \text{ AU} \left(\frac{\dot{M}}{10^{-8} M_\odot \text{ yr}^{-1}}\right)^{4/9} \left(\frac{M_*}{M_\odot}\right)^{1/3} \times \left(\frac{\alpha_{\text{mri}}}{0.02}\right)^{-1/5} \left(\frac{\kappa_D}{1 \text{ cm}^2 \text{ g}^{-1}}\right), \quad (5)$$

and

$$a_{\text{mstr}} = (1.06 \times 10^{-2} \text{ AU}) \beta' \left(\frac{R_*}{R_\odot}\right)^{12/7} \left(\frac{B_*}{1000 \text{ G}}\right)^{4/7} \times \left(\frac{M_*}{M_\odot}\right)^{-1/7} \left(\frac{\dot{M}}{10^{-7} M_\odot \text{ yr}^{-1}}\right)^{-2/7}, \quad (6)$$

where κ_D and B_* are the grain opacity and stellar magnetic field, respectively. With respect to spherical accretion, $\beta' = 1$ represents a typical Alfvén radius. The

variables $\alpha_{\text{dead}} = 0.001$ and $\alpha_{\text{mri}} = 0.01$ denote the value of α in the dead zone and in the active zone at the midplane of the disk, respectively.

Based on the above-described equations, we can calculate the gas density $\Sigma_g \propto r^{-1}$. The stellar accretion rate and stellar magnetic field are believed to be two important factors that affect the profile of the gas density (Wang et al. 2012). Therefore, in our model, we consider these parameters in the investigation of planet formation and test our simulations by varying them.

2.2. Eccentricity damping and planetary migration

For a planetary embryo embedded in a gas disk, mutual interactions will result in the eccentricity damping of the embryo on a timescale τ_{damp} represented as (Cresswell & Nelson 2006)

$$\tau_{\text{damp}} = \left(\frac{e}{\dot{e}}\right) = \frac{Q_e}{0.78} \left(\frac{M_*}{m}\right) \left(\frac{M_*}{a^2 \Sigma_g}\right) \left(\frac{h}{r}\right)^4 \Omega^{-1} \times \left[1 + \frac{1}{4} \left(e \frac{r}{h}\right)^3\right] \text{ yr}, \quad (7)$$

where $Q_e = 0.1$ is a normalized factor fitted to hydrodynamical simulation results and h , r , Ω , and e are the disk scale height, the distance from the central star, the Kepler angular velocity, and the eccentricity of the embryo, respectively.

Additionally, the angular momentum exchange between embedded planets and the gaseous disk will trigger orbital migration of the planets. According to the core-accretion scenario (Ida & Lin 2004), type I and type II migration are proposed to explain the formation of close-in super Earths or hot Jupiters.

If a planet embryo occupies a low mass ($\leq 30 M_\oplus$), the angular momentum exchange between the embryo and gaseous disk can be analyzed using a linear model, and the net loss from the embryo will eventually lead to an inward migration (Goldreich & Tremaine 1979; Ward 1997; Tanaka et al. 2002). The timescale for type I migration can be expressed as

$$\tau_{\text{migI}} = \frac{a}{|\dot{a}|} = \frac{1}{f_1(2.7 + 1.1\beta)} \left(\frac{M_*}{m}\right) \left(\frac{M_*}{\Sigma_g a^2}\right) \times \left(\frac{h}{a}\right)^2 \left[\frac{1 + \left(\frac{er}{1.3h}\right)^5}{1 - \left(\frac{er}{1.1h}\right)^4}\right] \Omega^{-1} \text{ yr}, \quad (8)$$

where e , r , h and Ω bear the same definition as in equation (7). The variable f_1 is the reduction factor. Using the gas-density profile given by equation (1), we have $\beta = -d \ln \Sigma_g / d \ln a = 1$.

In this work, we consider the gravitational interaction between each body in the system, type I migration (for planets with masses less than $30 M_\oplus$), and the eccentricity damping of the planets. The total acceleration of the planets with mass m_i is expressed as

$$\frac{d}{dt} \mathbf{v}_i = -\frac{G(M_* + m_i)}{r_i^2} \left(\frac{\mathbf{r}_i}{r_i}\right) + \sum_{j \neq i}^N G m_j \left[\frac{(\mathbf{r}_j - \mathbf{r}_i)}{|\mathbf{r}_j - \mathbf{r}_i|^3} - \frac{\mathbf{r}_j}{r_j^3} \right] + \mathbf{F}_{\text{damp}} + \mathbf{F}_{\text{migI}}, \quad (9)$$

where

TABLE 1
THE INITIAL PARAMETERS OF THE GROUPS IN CASE 1.

	Group 1	Group 2	Group 3	Group 4
Mass of planets (M_{\oplus})	(5, 10, 15)	(5, 5, 5), (5, 5, 10)	(2-30, 0.2-15, 0.5-22.5)	(5, 10, 15)
\dot{M} ($\times 10^{-8} M_{\odot} \text{yr}^{-1}$)	0.1-2.5	0.1-2.5	0.1-2.5	0.1, 0.5
B_* (KG)	0.5, 1, 1.5, 2, 2.5	0.5, 1, 1.5, 2, 2.5	0.5, 1, 1.5, 2, 2.5	0.5, 1, 1.5, 2, 2.5
f_1	0.01, 0.03, 0.1, 0.3, 1	0.01, 0.03, 0.1, 0.3, 1	0.01, 0.03, 0.1, 0.3, 1	0.01, 0.03, 0.1, 0.3, 1

TABLE 2
THE INITIAL PARAMETERS OF THE CASES IN CASE 2.

	A1	A2
Mass of planets inner (M_{\oplus})	2, 5	2, 5
Mass of planets outer (M_{\oplus})	5, 20	5, 20
\dot{M} ($\times 10^{-8} M_{\odot} \text{yr}^{-1}$)	0.1, 0.5, 2	0.1, 0.5, 2
B_* (KG)	0.5, 1	0.5, 1
f_1	0.03, 0.1	0.3, 1

$$\mathbf{F}_{\text{damp}} = -2 \frac{(\mathbf{V}_i \cdot \mathbf{r}_i) \mathbf{r}_i}{r_i^2 \tau_{\text{damp}}}, \quad (10)$$

$$\mathbf{F}_{\text{migI}} = -\frac{\mathbf{V}_i}{2\tau_{\text{migI}}},$$

where \mathbf{r}_i and \mathbf{V}_i represent the position and velocity vectors of planet m_i , respectively, and all of the vectors are expressed in stellar-centric coordinates.

To explore the dynamical evolution of the planets, we integrate equations (9) using the Hermit scheme (Aarseth 2003), which is a time-symmetric integrator.

For the numerical setup, we assume that the system contains a solar-mass central star with a surrounding gaseous disk. Initially, all of the planets should be in coplanar and near-circular orbits. The argument of the pericenter, the mean anomaly, and the longitude of ascending node are randomly generated to be between 0° to 360° . To examine the role of the stellar accretion rate, stellar magnetic field, the speed of the type I migration, and additional planets, we consider two cases with different initial parameters. For Case 1, we mainly investigate the configuration formation for three-planet systems with the various parameters we have chosen. For Case 2, we examine how additional planets affect the evolution of the system. In the following section, we will briefly introduce the main results obtained from the numerical simulations.

3. NUMERICAL SIMULATIONS AND RESULTS

3.1. Case 1

We mainly consider MMR formation in three-planet systems. In this case, we perform a total of 1020 runs. Furthermore, we choose three planets with variable masses for G1-G3, and we also change the initial locations for the planets for G4. Herein, we summarize each of the initial systems for G1-G4 that are adopted in the numerical simulations.

G1: In this group, given the isolation mass, the planet mass m is proportional to $a^{3/4}$. Therefore, the masses of the three planets are chosen to be 5, 10, and 15 M_{\oplus} (m1 labeled in panel (d) of Figure 2). For the first subgroup, the stellar accretion rate ranges from 0.1×10^{-8} to $2.5 \times 10^{-8} M_{\odot} \text{yr}^{-1}$, and f_1 varies from 0.01 to 1, whereas B_* always remains 0.5 KG in this subgroup. For

the second subgroup, we fix the stellar accretion rate at $0.1 \times 10^{-8} M_{\odot} \text{yr}^{-1}$, whereas the stellar magnetic field ranges from 0.5 to 2.5 KG, and f_1 varies from 0.01 to 1. The third subgroup is quite similar to the second subgroup except that the stellar rate remains $0.5 \times 10^{-8} M_{\odot} \text{yr}^{-1}$. In summary, we carry out a total of 90 runs for G1 (including three subgroups).

G2: For this group, three subgroups are also considered in the simulations. The initial parameters adopted are similar to the parameters adopted for G1 except for the planetary masses. The masses of the three planets are divided into two cases: (1) the three planets have an equal mass of 5 M_{\oplus} (m2 labeled in panel (d) of Figure 2) or (2) the inner two planets both bear a mass of 5 M_{\oplus} but the mass of the outer companion is 10 M_{\oplus} (m3 labeled in panel (d) of Figure 2). Additionally, the stellar accretion rate in subgroups 1, 2 and 3 is assumed to be 0.1×10^{-8} , 0.5×10^{-8} , 1×10^{-8} , 2×10^{-8} , and $2.5 \times 10^{-8} M_{\odot} \text{yr}^{-1}$, respectively. Herein, we perform 130 runs for G2.

G3: The statistical results (see Figure 1) show that most of the Kepler planets are in near-MMRs, particularly 3:2 and 2:1 MMRs. For three-planet systems, we classify the ratios of the planetary masses into four types: 1:1:1.5, 2:1:7.5, 12:1:0.2 and 2:0.2:4. For further investigation, we then choose six subgroups for three planets depending on the variable masses such that the combinations of the planetary masses are as follows: [5, 5, 7.5] M_{\oplus} (subgroup m4), [2, 1, 7.5] M_{\oplus} (subgroup m5), [30, 2.5, 0.5] M_{\oplus} (subgroup m6), [15, 15, 22.5] M_{\oplus} (subgroup m7), [6, 3, 22.5] M_{\oplus} (subgroup m8) and [2, 0.2, 4] M_{\oplus} (subgroup m9). Herein, the stellar accretion rates are assumed to be 0.1×10^{-8} , 0.5×10^{-8} , 1×10^{-8} , 2×10^{-8} , and $2.5 \times 10^{-8} M_{\odot} \text{yr}^{-1}$, respectively, whereas other the initial parameters are similar to the parameters assumed for G1, except for the planetary masses. Therefore, we carry out 750 runs for G3.

G4: To determine the likelihood that there is a high proportion of planet pairs near 3:2 MMR, we reset the initial locations of the three planets, which differ greatly from the locations considered in G1-G3. We also choose five subgroups for the stellar accretion rate (as performed for G1-G3), and the stellar magnetic field is set at 0.5, 1, 1.5, 2, and 2.5 G. The masses of the three planets are exactly equal to the masses in G1. For this group, 50 runs are carried out in the simulations.

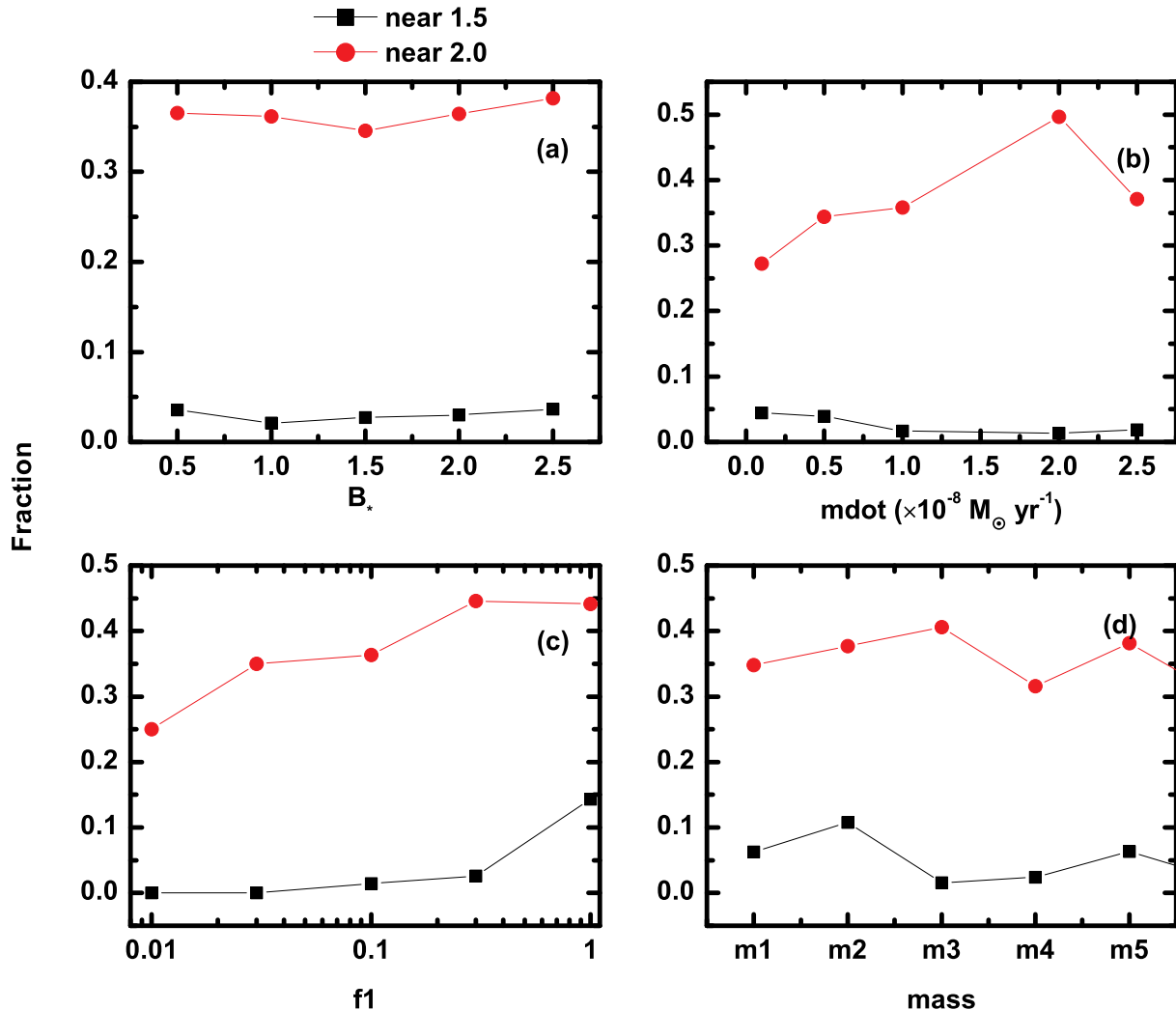


FIG. 2.— The statistic results of all runs in G1-G3. Panel (a) shows the distribution of period ratio with different star magnetic field fixed and other parameters are free. The black square represents the planet pairs near 3:2 MMR and the red circle means the statistics of planet pairs near 2:1 MMR. Panel (b) shows the results with different star mass accretion rate. Panel (c) displays the results of different speed of type I migration, and panel (d) represents the fraction of the period ratio varies with the masses of the three planets.

For each of the above mentioned runs, we performed the simulation over a timescale of 5 Myr. In the following section, we will concisely summarize the most significant results obtained from our numerical simulations.

3.1.1. Statistic outcomes for G1-G3

In groups G1-G3, the three planets possess orbital periods of 100, 250, and 600 days for f_1 in the range of [0.01, 0.03], and 140, 500, and 1450 days for $f_1 \geq 0.1$ initially.

From the statistical results obtained for G1-G3, we observe that the proportion of planet pairs near a 2:1 MMR is approximately 36.4%, with the period ratio ranging from 1.83 to 2.18. However, the proportion of planet pairs near a 3:2 MMR is approximately 3.0%, with the period ratios in the range of [1.45, 1.54]. Figure 2 shows the statistical results obtained for period ratios near 1.5 and 2.0, and panels (a), (b), (c) and (d) present the results obtained by considering variations in the stellar magnetic field, stellar mass accretion rate, the speed of the type I migration, and the planet mass. Based on Fig-

ure 2, we may conclude that it is difficult for two planets to be trapped near a 3:2 MMR under such a formation scenario. However, two planets can be easily captured in a 2:1 MMR. Hence, it is inevitable for three planets to be trapped in 4:2:1 MMR through the aforementioned formation scenario based on our model.

Panel (a) of Figure 2 displays the statistics for periods near 1.5 and 2.0 with different stellar magnetic field. The red dotted line represents the results obtained near a period ratio of 2.0, whereas the line composed of black squares represents the results obtained near 1.5. Based on the results presented in panel (a), we can conclude that the proportion corresponding to approximately 2.0 is largest for $B_* = 2.5$, whereas for $B_* = 0.5$ and 2.5 the proportion near 1.5 is nearly the same, which is the highest value obtained among the five scenarios. The proportion changes slightly with an increase in the magnetic field, which enables us to conclude that the stellar magnetic field plays a less significant role in the formation of 2:1 or 3:2 MMRs over the evolution of the system.

Panel (b) shows that, for the formation of 2:1 MMRs,

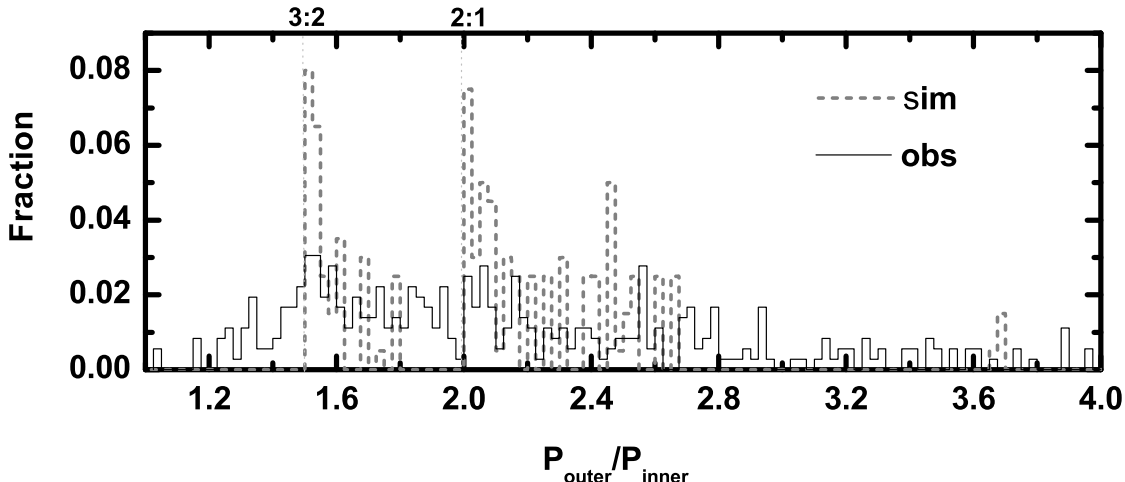


FIG. 3.— The statistic results of observation of three-planet systems and simulation results from 50 runs in G1 and 50 runs in G4. The black solid line means the observation results and the grey dot represents the simulation results in G1 and G4.

the $\dot{M} = 2 \times 10^{-8} M_{\odot} \text{ yr}^{-1}$ values are larger than the values observed in other cases. Thus, $\dot{M} = 2 \times 10^{-8} M_{\odot} \text{ yr}^{-1}$ is the most favorable value for producing 2:1 MMRs. To yield 3:2 MMRs, this proportion becomes greatest when $\dot{M} = 0.1 \times 10^{-8} M_{\odot} \text{ yr}^{-1}$, as shown in Figure 2. Therefore, 2:1 MMRs can form easily during the early stages of star formation with a high mass accretion rate, whereas 3:2 MMRs can form easily during the late stages of star formation. In cases in which the stellar accretion rate remains unaltered, we also notice that several planet pairs are trapped near higher-order MMRs of approximately 5:3, 5:2 and 3:1. Furthermore, $\dot{M} = 0.1 \times 10^{-8} M_{\odot} \text{ yr}^{-1}$ is propitious for the formation of planet pairs near 5:2 and 3:1 MMRs.

Panel (c) of Figure 2 shows the proportions of planet pairs with different migration speeds. Based on the results presented in Figure 2, we can determine that the proportion of planet pairs near a 2:1 MMR is greater than 35% for $f_1 = 0.1, 0.3$, and 1, and we also find that the proportion of planet pairs near a 3:2 MMR is greater than 2.5% for $f_1 \geq 0.3$, and greater than 10% for $f_1 = 1$. Therefore, $f_1 \geq 0.1$ appears to favor planetary configurations near-2:1 MMRs, which is consistent with the work of Ida & Lin (2008), Wang & Zhou (2011) and Wang et al. (2012). However, $f_1 \geq 0.3$ is propitious for the formation of near-3:2 MMRs. We also note that $f_1 = 0.03$ facilitates the capture of two planets in near-3:1 MMRs.

From panel (d) of Figure 2, we observe that the proportion of planet pairs forming near-2:1 MMRs is greater than 30.0% for the five scenarios, where subgroup m3 with the inner two planets being of equal mass bears the largest proportion. For planet pairs forming near-3:2 MMRs, the situation in which there are three equal-mass planets, demonstrates the largest proportion. These results indicate that two planets are easily involved in or are near a first-order MMR if they have equal masses.

3.1.2. Statistical outcomes for G4

In G1-G3, the period ratios of the three planets are initially set to be greater than 2.0. From the results given in Section 3.1.1, we note that the fraction of planet pairs with period ratio near 1.5 from the simulations is lower than that from the observation. Therefore, in G4, we set the systems with a compact structure by varying the initial orbits of the three planets with the period ratio, which ranges between 1.5 and 2.0, at 140, 270, and 530 days initially. Thus, we perform 50 runs for G4 with those parameters in Table 1. In these simulations, the planetary masses are adopted to be 5, 10 and 15 M_{\oplus} , which are identical to those in G1.

Upon the completion of the simulations, we collect the data obtained from G4 (50 simulations with the initial parameters given in Table 1) and G1 (50 simulations with identically initial parameters of the stellar magnetic field, the stellar accretion rate, and the reduce factor of type I migration as in G4, but with various initial locations), and the simulation results of the 100 simulations are plotted to compare them with the observations.

The statistical results are shown in Figure 3. The black solid line in this figure denotes the distribution profile of the Kepler observations, whereas the grey dot represents the results of our simulations. In Figure 3, we note that there exist two peaks near 1.5 and 2.0 from the numerical simulations that are consistent with the observations. The proportion of planet pairs near 1.5 and 2.0 is approximately 14.5% and 26.0%, respectively. Compared with the results obtained for G1-G3 (see Figure 2), we find that the proportion near 1.5 increases, whereas the proportion near 2.0 decreases. Furthermore, we notice that a lower proportion peak emerges near 2.5 (5:2 MMR), but the planet pair is absent at 3:1 MMR due to the limited number of simulations performed. Moreover, we perform a KS test on the distributions, we find that the p-value $p = 0.06$ for $\dot{M} = 0.1 \times 10^{-8} M_{\odot} \text{ yr}^{-1}$ when the simulations compare with the observation data, implying that they roughly have similar distribution. Consequently, we conclude that the formation scenario proposed in this

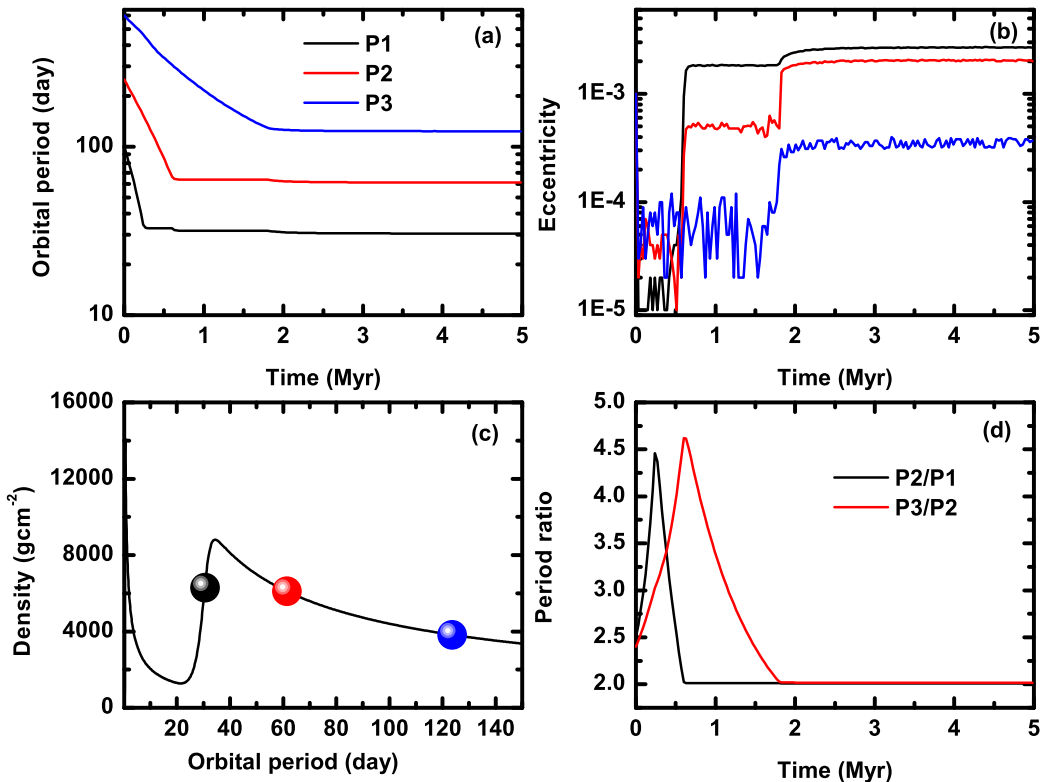


FIG. 4.— Results for R1. Panels (a), (b) and (d) show the evolution of orbital period, eccentricity, and period ratio of planets pair, respectively. Panel (c) shows the final configuration of three planets. P1, P2, and P3 represent the innermost, the intermediate and the outermost planet, respectively. The black solid curve is the density profile of the gas disk initially.

work may reproduce a subset of the planet pair distributions.

3.1.3. R1: Two pairs of planets both in 2:1 MMR

In this run, the initial parameters (see Table 3) are assumed to be as follows: the masses of three planets are identically set to be $5 M_{\oplus}$; the stellar accretion rate is adopted to be $1 \times 10^{-8} M_{\odot} \text{ yr}^{-1}$, which indicates a middle stage for the star formation; the stellar magnetic field is 0.5 KG; and the reduction factor f_1 is 0.03, implying a slow speed of type I migration. Based on the simulation results, we find that the three planets are trapped in 4:2:1 MMRs in 9.5% of all simulations.

Figure 4 shows the typical evolution leading to the formation of a Laplacian configuration. Panels (a) and (b) show the dynamical behavior of the semi-major axes and eccentricities over a timescale of 5 Myr. After the planets are captured in the resonances, the semi-major axes remain nearly unchanged while the eccentricities approach zero; here, the black, red and blue lines represent the innermost, intermediate and outermost planets, respectively. In addition, the trio’s final configuration is clearly shown in panel (c), which is indicative of the relationship between the final orbits (denoted by the orbital periods) and the gas density profile. Moreover, panel (d) shows the variations in the period ratio of two planet pairs. Furthermore, in Figure 4, we note that the innermost planet reaches the maximum gas density very quickly at ~ 0.2

Myr, and the inner two planets are locked in a 2:1 MMR at ~ 0.6 Myr at the time the second planet arrives, but the outer two planets are in a 2:1 MMR at ~ 1.8 Myr. Again, based on panel (c), we observe that the inner two planets cease migrating in the regime in which the gas density nearly reaches its maximum, and the outer two companions also stop moving inward, following the behavior of the inner two. Ultimately, the three planets stop migrating at orbital periods of 30.5, 61.3 and 123.6 days, from innermost to outermost. The planets’ eccentricities are damped due to the high density of the gas disk. Such a configuration is reminiscent of the KOI-1426 system, which also consists of three planets with orbital periods of 38.9, 74.9 and 150.0 days, from innermost to outermost, indicating that the system may be captured into Laplacian resonance during dynamical evolution.

3.1.4. R2: The inner pair is in a 3:2 MMR, whereas the outer pair is in a 2:1 MMR

In R2, the masses of the three planets are 5, 10 and $15 M_{\oplus}$, the stellar accretion rate is $0.1 \times 10^{-8} M_{\odot} \text{ yr}^{-1}$, and the stellar magnetic field is 1 KG. The speed of the type I migration is equal to unity, which is consistent with linear theory (Goldreich & Tremaine 1979; Ward 1997; Tanaka et al. 2002).

Based on the statistics obtained, we find that approximately 2.2% of the total simulations are associated with the final configurations in which the inner two planets

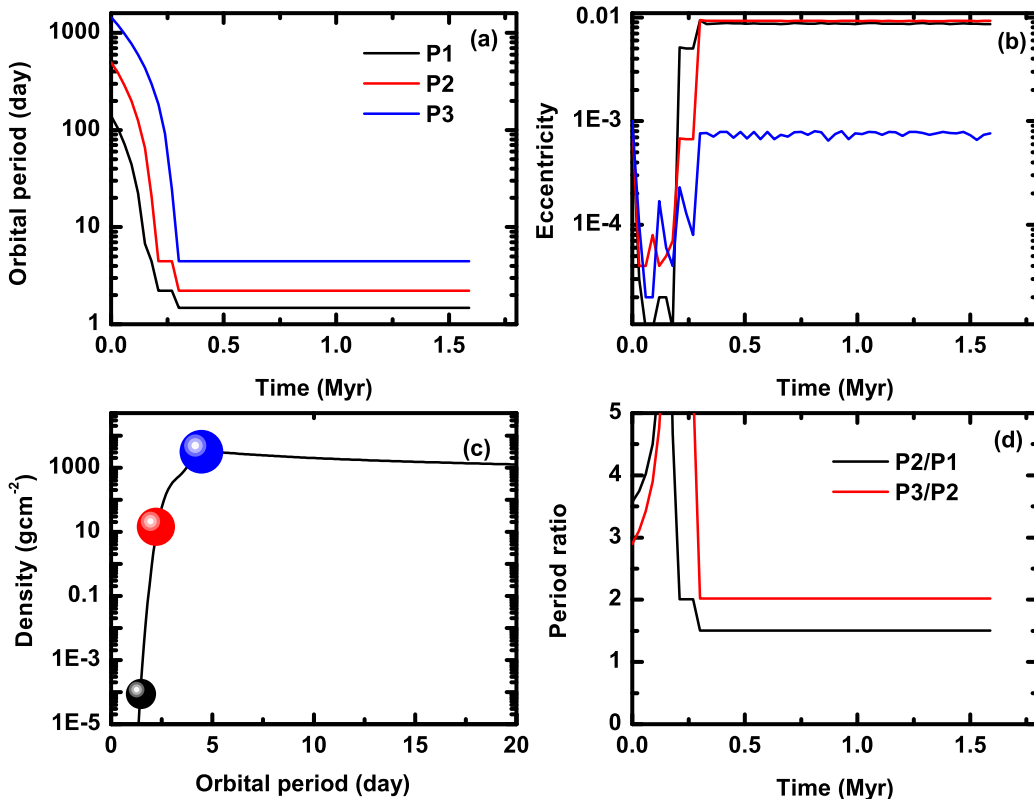


FIG. 5.— Results for R2. Panels (a), (b), and (d) show the evolution of orbital period, eccentricity, and period ratio of the planet pair, respectively. Panel (c) shows the final configuration of three planets. P1, P2, and P3 denotes the innermost, the intermediate and the outermost planet, respectively. The black solid curve is the density profile of the gas disk initially.

TABLE 3
THE INITIAL PARAMETERS OF R1, R2, R3 AND R4.

	R1	R2	R3	R4
Mass of planets (M_{\oplus})	5, 5, 5	5, 10, 15	5, 5, 5	5, 5, 7.5
\dot{M} ($\times 10^{-8} M_{\odot} \text{yr}^{-1}$)	1	0.1	1	0.1
B_* (KG)	0.5	1	0.5	1.5
f_1	0.03	1	0.3	1

are in a 3:2 MMR, whereas the outer two are trapped in a 2:1 MMR. Figure 5 shows the outcomes for a typical case. Similar to Figure 4, panels (a) and (d) show that the inner two planets are locked in a 2:1 MMR at ~ 0.2 Myr initially. Subsequently, when the third planet P3 approaches P2, the 2:1 MMR is disrupted, and the inner pair is then trapped in a 3:2 MMR at ~ 0.3 Myr, while the outer two companions enter a 2:1 MMR. Furthermore, panel (c) shows that the three planets can travel across the region where the density reaches its maximum. In addition, the outermost planet simply halts its migration in the scenario in which the density is maximal. Moreover, the results show that the eccentricities of the inner pair can be excited to 0.01 when they enter a 2:1 MMR, and the outermost planet’s eccentricity is slightly increased to 0.001 in the case of the arrival at resonance, which is different from the case of R1. At the end of the simulation, the three planets hold orbital periods of 1.5, 2.2 and 4.5 days. We also observe a comparable analogy among the Kepler candidates KOI-584, with orbital

periods of 6.5, 9.9 and 21.2 days, from innermost to outermost, by considering the orbital period ratios of the planet pairs.

3.1.5. R3: Two planet pairs both in 3:2 MMR

In R3, we assume the parameters are as follows: the masses of the three planets are all equal to $5 M_{\oplus}$, and the stellar accretion rate and stellar magnetic field share identical values with the values considered in R1. However, the speed of the type I migration is 0.3, ten times the speed considered in R1.

In this case, in 0.65% of all of the simulations, both of the two-planet pairs are captured in 3:2 MMRs. Figure 6 shows that the inner pair falls into a 3:2 MMR quickly. Subsequently, when P3 arrives, the inner and outer pairs both evolve into 3:2 MMRs. We note that the innermost planet travels across the region of maximum density, whereas the other two planets remain in the region where the gas density remains high. However, we note that the planets’ eccentricities are excited not

far from zero, decreasing to 0.002-0.008 during their evolution. In summary, we can conclude that rapid type I migration drives the three planets toward 3:2 MMRs, with the orbital periods of the planets being 20.9, 31.5 and 47.5 days. In this case, no comparable planetary analog of the Kepler candidates is found.

3.1.6. R4: *The inner pair is in a 2:1 MMR, whereas the outer pair is in a 3:2 MMR*

In the numerical simulations performed for R4, we consider the masses of the three planets to be 5, 5 and 7.5 M_{\oplus} , and the stellar accretion rate and reduction factor of the type I migration are equal to the values considered in R2. The stellar magnetic field is 1.5 KG, higher than the value considered in R2, resulting in a larger inner hole in the gas disk.

In this group, we notice that 0.32% of all simulations consist of a 2:1 MMR for the inner pair and a 3:2 MMR for the outer pair. Therefore, the three companions are locked in the chain of a 3:2:1 MMR. Figure 7 shows one of the typical simulations. Figure 7 shows that the inner pair first falls into a 2:1 MMR at ~ 0.4 Myr. When the planets are trapped in a 2:1 MMR, their eccentricities are increased to ~ 0.1 but then are dissipated by the gaseous disk within 1 Myr. In addition, we find that the occurrence of P3 indeed triggers the capture of the two outer planets in a 3:2 MMR, thereby leading to a 3:2:1 MMR for the three companions. During their evolution, the three planets move across the region of maximum density and reach the inner hole of the system, with final orbital periods of 1.5, 3.0 and 4.7 days. This configuration bears a resemblance to the KOI-1835 system, with three planets exhibiting orbital periods of 2.2, 4.6 and 6.8 days.

3.2. Case 2

Based on the results obtained for G1-G3, we note that the proportion of planet pairs near 2:1 MMRs is greater than that of planets near 3:2 MMRs when we compare the histogram of the numerical results with the observations. Thus, a question arises: Is there any likelihood that the occurrence of additional planets may contribute to the dynamical evolution of planet pairs in the existing systems over secular timescales, which could explain the difference between the simulations and observations? To address this question, we perform further numerical simulations, initially placing one or more additional planets into the previous systems that could be trapped in 2:1 and 3:2 resonances during their evolution. Based on the results obtained for Case 1, the systems involved in 2:1 and 3:2 MMRs are ultimately chosen for further investigation (see Table 2), for which it is assumed that the companions settle into either the closest or the most distant orbits from the central star. In this case, we perform a total of 24 runs in the simulation, with the systems divided into the two groups: A1 and A2.

A1: For this group, we investigate how additional planets may affect the planets captured in or near 2:1 MMRs during their evolution. For the initialization of the numerical simulations, three subgroups are considered: (1) a planet with a mass of 2 or 5 M_{\oplus} is assumed to be inside the orbit of the innermost planet; (2) a planet with a mass of 5 or 20 M_{\oplus} is located outside the orbit of the outermost planet; (3) two planets are, respectively, placed

inside the orbit of the innermost planet and outside the orbit of the outermost planet in the system (Table 2).

A2: For this group, we explore the issue of how additional planets stir up 3:2 MMR systems. For a detailed study, we also classify the simulations into three subgroups, similar to those case of A1. In the following section, we briefly summarize the major results.

3.2.1. The results of A1-A2

Panels (a), (b) and (c) in Figure 8 show the variations in the period ratios for a typical run in A1, where E1 represents the added planet residing inside the orbit of the innermost planet and E2 denotes the planet inserted outside the orbit of the outermost planet. As previously mentioned, the adopted three-planet system can form a configuration approximating a 4:2:1 MMR in Case 1, with a stellar accretion rate of $2 \times 10^{-8} M_{\odot} \text{ yr}^{-1}$, a stellar magnetic field of 0.5 KG, and a reduction factor of 0.03. As shown in Figure 8, E1 and E2 do not disrupt the 4:2:1 MMR in the original system, indicating that Laplacian resonance is very robust. Panels (a) and (b) exhibit orbital period ratios of P1/E1=1.5 and E2/P3=1.5, respectively, which suggests that E1 or E2 has a good probability of entering into a 3:2 MMR with the nearby planet (herein P1 or P3, respectively).

Panel (c) shows that E1 and P1 are captured in 3:2 resonance within a very short timescale, whereas E2 and P3 are locked into 3:2 resonance over a much longer timescale, approximately ~ 2 Myr. However, it is noteworthy that the resultant configuration of the 3:2:1 MMR is produced for the three planets E2, P3 and P2. Fortunately, we find that the system KOI-2433, consisting of four low-mass planets, bears resemblance to the configuration shown in panel (a), where their orbital periods are 10.0, 15.2, 27.9 and 56.4 days, from innermost to outermost. Again, this finding further indicates that the formation scenario may be applicable to other Kepler systems that are close to 3:2:1 MMRs.

In Figure 8, panels (d), (e) and (f) show the typical period ratio in A2. In this run, a three-planet system with a stellar accretion rate of $2 \times 10^{-8} M_{\odot} \text{ yr}^{-1}$, a stellar magnetic field of 0.5 KG, and a reduction factor of 0.3 in Case 1 can form a configuration in which both of the planet pairs are in near-3:2 MMRs. Panel (d) shows that the E1 and P1 pair is temporarily trapped in 3:2 resonance; thus, the two planets are ultimately locked into a 2:1 resonance, whereas P2 and P1 subsequently enter into a 3:2 MMR; however, the resonance is disrupted within 1 Myr, and the two outer planets P3 and P2 continue to evolve into a 3:2 resonance.

Panel (e) illustrates that P2 and P1 first undergo a 3:2 resonance within 0.1 Myr, and then P3 and P2 are locked into this resonance, which is held for a short period of time. Subsequently, the 3:2 MMRs for the two pairs (P2, P1) and (P3, P2) are both disrupted owing to the existence of the additional planet E2. Finally, P2 and P1 enter into an alternative 2:1 resonance during their dynamical evolution, whereas E2 and P3 are eventually locked into a 3:2 resonance. Panel (f) shows that the three pairs of (P1, E1), (P2, P1) and (P3, P2) are temporarily in 3:2 MMRs over the course of their evolution, but ultimately, only the outer pair of (E2, P3) is captured in 3:2 resonance.

Based on the above-described results, we conclude that

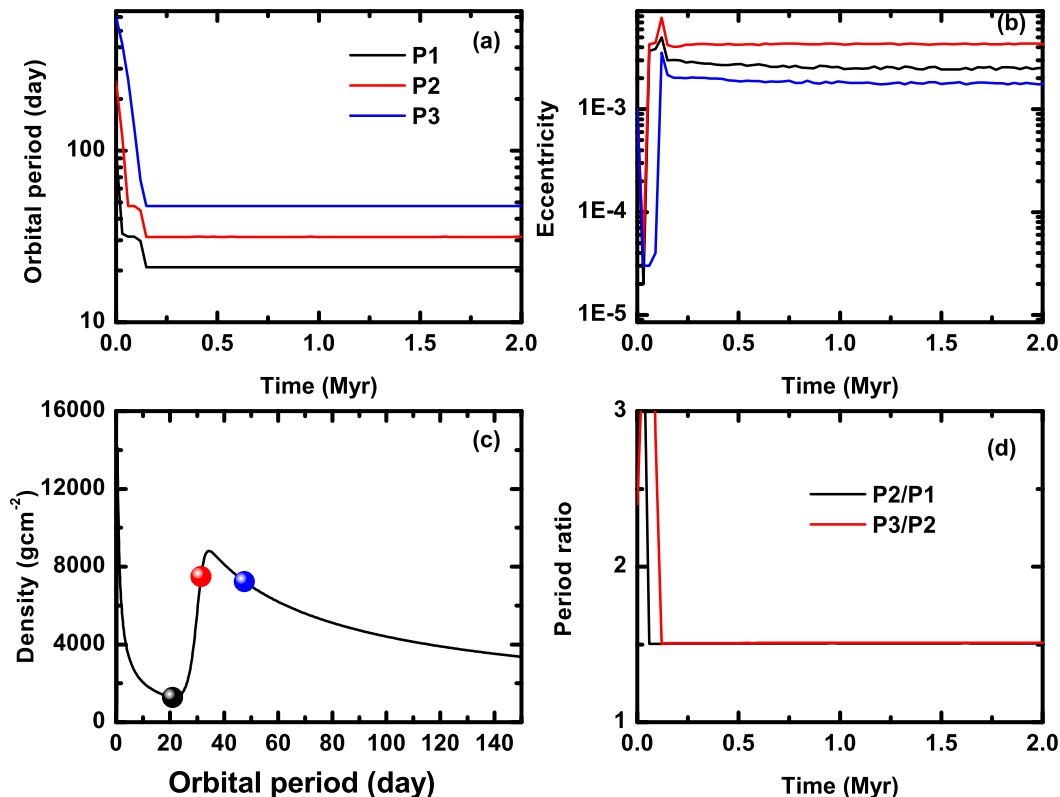


FIG. 6.— Results for R3. Panels (a), (b), and (d) show the evolution of orbital period, eccentricity, and period ratio of planets pair, respectively. Panel (c) shows the final configuration of three planets. P1, P2 and P3 stand for the innermost, the intermediate and outermost planet, respectively. The black solid curve is the density profile of the gas disk initially.

Laplacian resonance is not easily disrupted by additional planets, and the additional planets will lead to the formation of 3:2 MMRs; however, for planetary systems that are originally in two 3:2 MMRs during their evolution, the 3:2 resonance will disintegrate due to the interplay of planets.

4. CONCLUSIONS AND DISCUSSIONS

In this work, we extensively investigated the planetary configuration formation of systems that are involved in first-order resonances (e.g., 2:1 and 3:2 MMRs) via numerical simulations. In total, we performed over 1000 runs, considering systems with various combinations of planetary mass, stellar accretion rate, stellar magnetic field, speed of type I migration and additional planets. Moreover, we also compared our numerical results with the planetary candidates released by the Kepler mission. We summarize the major conclusions of our study as follows.

- Concerning the statistics of the observed data, the proportion of planet pairs near 2:1 MMRs is $\sim 18.0\%$ for three-planet systems. However, our numerical simulations show that the proportion of planet pairs in 2:1 MMRs remains 36.4% for G1-G3 and 26.0% for G4. Apparently, near 2:1 MMR configuration can be formed easily (Lee & Peale 2002) through our formation scenario and it is able to yield a proportion of planet pairs captured in 2:1 MMRs that is similar to the observed proportions and should thus provide an explanation of the

behavior of Kepler candidates involved in 2:1 MMRs.

With respect to 3:2 MMRs, the observation results yielded by the Kepler mission show that the proportion of planet pairs in this MMR is $\sim 7.0\%$ for three-planet systems. In contrast, this proportion can reach up to 14.5% in our simulations due to the original packed configuration of the systems. This formation scenario also sheds light on the generation of 3:2 resonant configurations in Kepler systems.

From our simulations, we get two peak-trough features at 3:2 and 2:1 MMRs which can be seen from the observation data. In this work, we focus on the planets with mass smaller than $30 M_{\oplus}$. Thus, we believe that the scenario with migrating planets is effective for the formation of near MMRs configuration for low mass planets (Libert & Tsiganis 2011). While for massive planets, with a mass larger than $20 M_{\oplus}$, the two peak-trough features can be reproduced using in situ formation scenario with growing planets (Petrovich et al. 2013).

- The formation of MMRs does not appear to be sensitive to the stellar magnetic field.

- Moreover, we find that $\dot{M} = 2 \times 10^{-8} M_{\odot} \text{ yr}^{-1}$, corresponding to the early stages of star formation, is conducive to 2:1 MMR formation for two planets, whereas $\dot{M} = 0.1 \times 10^{-8} M_{\odot} \text{ yr}^{-1}$, which is indicative of the late stages of star formation, contributes greatly to 3:2 MMR formation.

- Our simulations also suggest that $f_1 \geq 0.1$ is a

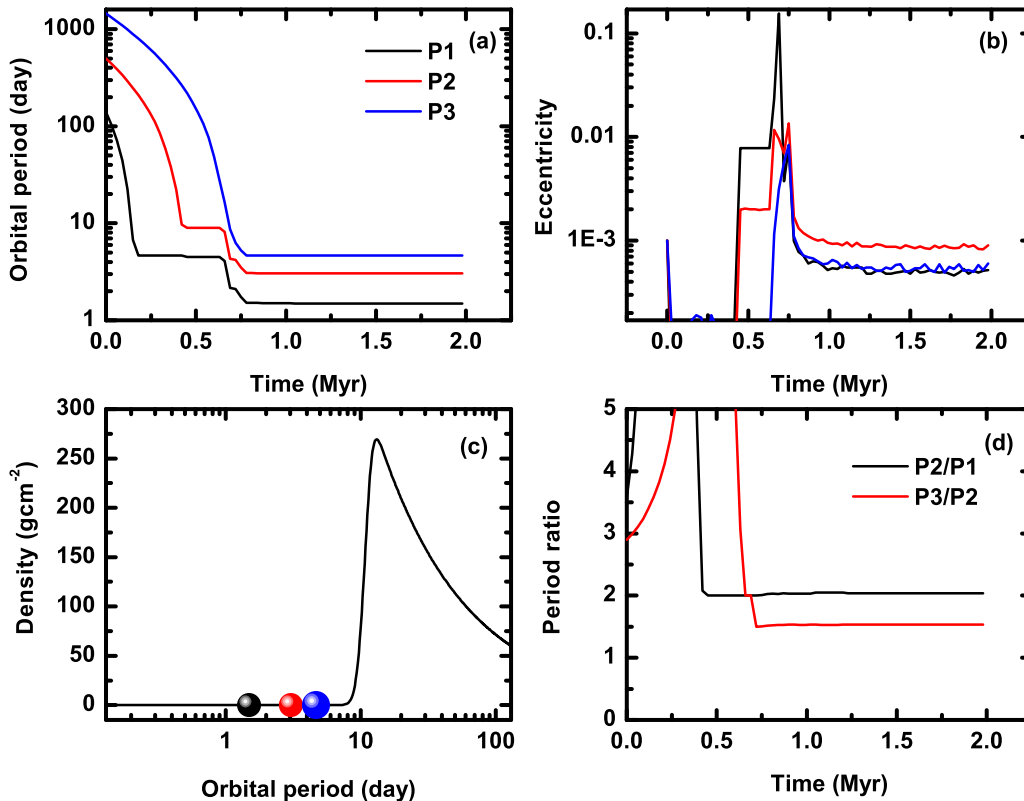


FIG. 7.— Results for R4. Panels (a), (b) and (d) show the dynamical evolution of orbital period, eccentricity and period ratio of the planet pairs, respectively. Panel (c) shows the final configuration of three planets. Herein P1, P2 and P3 denotes the innermost, the intermediate and the outermost planet, respectively. The black solid curve is the density profile of the gas disk initially.

proper value for the speed of type I migration that may result in the formation of near-2:1 MMRs, which is consistent with our previously reported results (Wang et al. 2012), whereas $f_1 \geq 0.3$ appears to favor the production of planet pairs in near-3:2 MMRs. To summarize, a slower speed of type I migration (as low as one-tenth the theoretical value) plays a vital role in the resonance formation of systems.

The 1:2:4 and 1:2:3 MMRs usually formed when the first planet is trapped in the edge of the holes in the gas disk. The formation scenario is similar to that mentioned in Pierens & Nelson (2008), the MMR formed when the planet is captured in the gap of another planet.

Furthermore, compared with our previous work, herein, we have not explored tidal interactions between a central star and its planets (Lithwick & Wu 2012; Batygin & Morbidelli 2013). In the present work, we merely consider planets with a mass of less than $30 M_{\oplus}$ based on a tidal timescale (Mardling & Lin 2004; Zhou & Lin 2008), under which the planets' semi-major axes and eccentricities will gradually decrease but the period ratios will change little due to tidal effects. In fact, tidal interactions would trigger the degradation of first-order resonance systems to near-resonance systems (Lee et al. 2013).

In summary, we conclude that the near-MMR configurations such as those exhibited by Kepler candidates could be produced under this formation scenario. In addition, our investigation may reveal that this formation scenario is not only applicable to Kepler systems but is also suitable for other planetary systems, especially for systems composed of several short-period planets with low masses. In this respect, our work should shed new light on the planetary formation of such systems in general.

We thank the referee for the constructive comments that helped to improve the original content of this manuscript. W.S. and J.J.H. are supported by National Natural Science Foundation of China (Grants No. 11273068, 11203087, 11473073), the Strategic Priority Research Program-The Emergence of Cosmological Structures of the Chinese Academy of Sciences (Grant No. XDB09000000), the innovative and interdisciplinary program by CAS (Grant No. KJZD-EW-Z001), the Natural Science Foundation of Jiangsu Province (Grant No. BK20141509), and the Foundation of Minor Planets of Purple Mountain Observatory.

REFERENCES

Aarseth, S. J. 2003, *Gravitational N-Body Simulations*, by Sverre J. Aarseth, pp. 430. Cambridge, UK: Cambridge University Press, November 2003.

Batalha, N. M., Rowe, J. F., Bryson, S. T. et al. 2013, *ApJS*, 204, 24

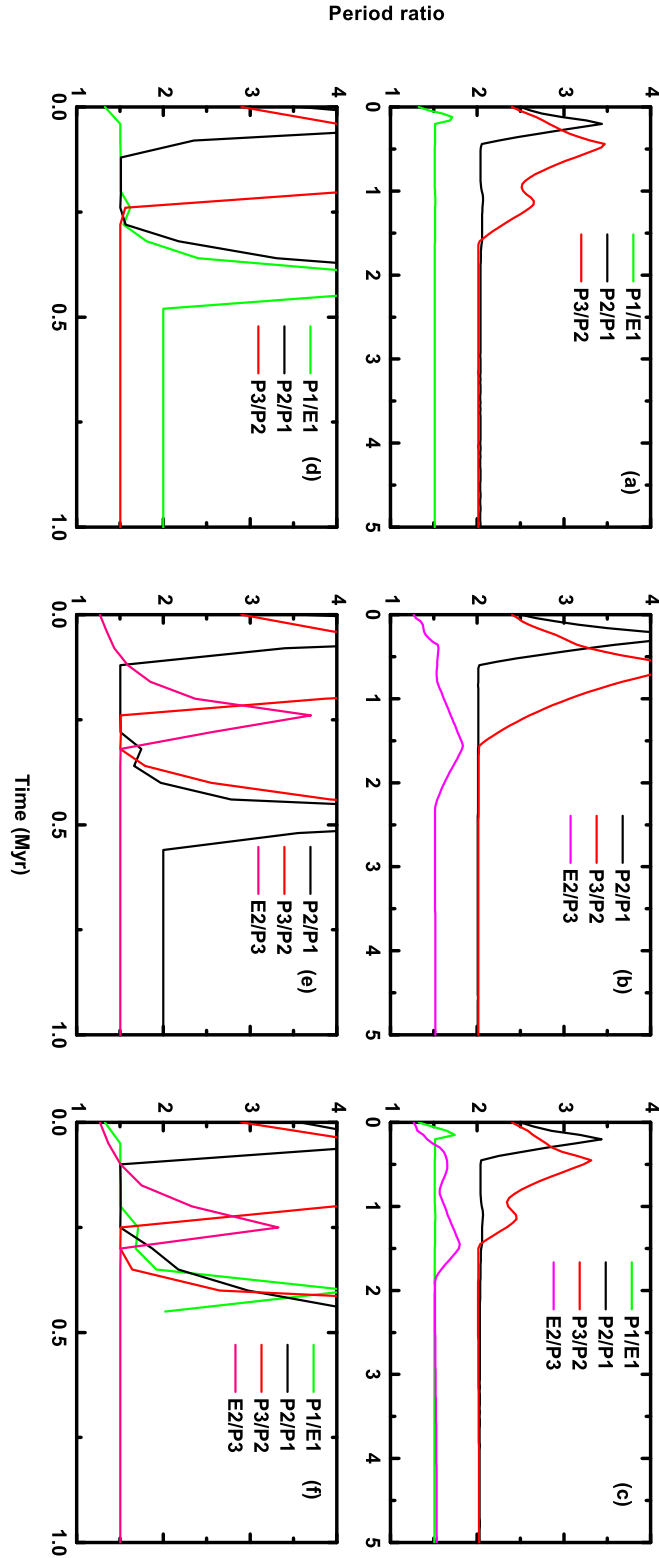


FIG. 8.— Evolution of period ratios for A1 and A2. Panels (a), (b) and (c) show the evolution of period ratio of planet pair for A1, respectively. Panels (d), (e) and (f) exhibit the cases of A2, respectively. Herein E1 represents the supposed planet inhabits inside the innermost planet, and E2 denotes the additional planet resides beyond the outermost planet. The green, black, red and pink lines show the period ratios of P1/E1, P2/P1, P3/P2 and E2/P3, respectively.

- Batygin, K., & Morbidelli, A. 2013, *AJ*, 145, 1
- Bryden, G., Rozyczka, M., Lin, D. N. C., & Bodenheimer, P. 2000, *ApJ*, 540, 1091
- Ciardi, D. R., et al. 2013, *ApJ*, 763, 41
- Cresswell, P., & Nelson, R. P. 2006, *A&A*, 450, 833
- Fabrycky, D. C., Lissauer, J. J., Ragozzine, D., et al. 2012, arXiv:1202.6328
- Goldreich, P., & Tremaine, S. 1979, *ApJ*, 233, 857
- Goldreich, P., & Tremaine, S. 1980, *ApJ*, 241, 425
- Haisch, K. E., Jr., Lada, E. A., & Lada, C. J. 2001, *ApJ*, 553, L153
- Hayashi, C. 1981, *Prog. Theor. Phys. Suppl.*, 70, 35
- Howard, A. W. 2013, *Science*, 340, 572
- Ida, S., & Lin, D. N. C. 2004, *ApJ*, 604, 388
- Ida, S., & Lin, D. N. C. 2008, *ApJ*, 673, 487
- Ji, J., Li, G., & Liu, L. 2002, *ApJ*, 572, 1041
- Ji, J., Liu, L., Kinoshita, H., et al. 2003, *ApJ*, 591, L57
- Koenigl, A. 1991, *ApJ*, 370, L39
- Kretke, K. A., & Lin, D. N. C. 2007, *ApJ*, 664, L55
- Kretke, K. A., Lin, D. N. C., Garaud, P., & Turner, N. J. 2009, *ApJ*, 690, 407
- Libert, A.-S., & Tsiganis, K. 2011, *CeMDA*, 111, 201
- Lissauer, J. J., Ragozzine, D., Fabrycky, D. C., et al. 2011, *ApJS*, 197, 8
- Lissauer, J. J., Marcy, G. W., Rowe, J. F., et al. 2012, *ApJ*, 750, L112
- Lithwich, Y. & Wu, Y. 2012, *ApJ*, 756, L11
- Lee M. H., & Peale S. J. 2002, *ApJ*, 567, 596
- Lee M. H., Fabrycky, D., & Lin D. N. C., 2013, *ApJ*, 774, 52L
- Lin, D. N. C., Bodenheimer, P., & Richardson, D. C. 1996, *Nature*, 380, 606
- Malhotra, R. 1995, *AJ*, 110, 420.
- Marcus, R. A., Sasselov, D., Hernquist, L., & Stewart, S. T. 2010, *ApJ*, 712, L73
- Masset, F., & Snellgrove, M. 2001, *MNRAS*, 320, L55
- Mardling, R. A., & Lin, D. N. C. 2004, *ApJ*, 614, 955
- Mazeh, T., et al. 2013, *ApJS*, 208, 16
- Natta, A., Testi, L., & Randich, S. 2006, *A&A*, 452, 245
- Ogihara, M., & Kobayashi, H., 2013, *ApJ*, 775, 34.
- Petrovich, C., Malhotra, R., & Tremaine, S. 2013, *ApJ*, 770, 24.
- Pringle, J. E. 1981, *ARA&A*, 19, 137.
- Pierens, A., & Nelson, R. P. 2008, *A&A*, 482, 333.
- Quillen, A. C., Bodman, E., & Moore, A. 2013, *MNRAS*, 435, 2256.
- Tanaka, H., Takeuchi, T., & Ward, W. R. 2002, *ApJ*, 565, 1257
- Valencia, D., O'Connell R. J., & Sasselov, D. 2006, *Icarus*, 181, 545
- Valencia, D., Sasselov, D., & O'Connell R. J., 2007, *ApJ*, 665, 1413
- Vorobyov, E. I., & Basu, S. 2009, *ApJ*, 703, 922
- Ward, W. R. 1997, *Icarus*, 126, 261
- Wang, S., & Zhou, J. L. 2011, *ApJ*, 727, 108
- Wang, S., Ji, J., & Zhou, J. L., 2012, *ApJ*, 753, 170
- Zhang, N., Ji, J., & Sun, Z. 2010, *MNRAS*, 405, 2016
- Zhou, J. L., Aarseth, S. J., Lin, D. N. C., & Nagasawa, M. 2005, *ApJ*, 631, L85
- Zhou, J. L., & Lin, D. N. C. 2008, *IAU Symposium*, 249, 285